G2 Study of the Triplet and Singlet $[H_3, P_2]^+$ Potential Energy Surfaces. Mechanisms for the Reaction of $P^+(^1D,^3P)$ with PH_3

Elso M. Cruz,† Xabier Lopez, Mirari Ayerbe, and Jesus M. Ugalde*

Kimika Fakultatea, Euskal Herriko Unibertsitatea, P.K. 1072, 20080 Donostia, Euskadi, Spain

Received: August 5, 1996; In Final Form: October 25, 1996[⊗]

A study of both the singlet and triplet potential energy surfaces of the $[H_3, P_2]^+$ system has been carried out using the G2 procedure. Various stable structures along with a number of reaction mechanisms for the reaction of both the ^1D and ^3P electronic states of P^+ with phosphine have been elucidated. The most stable isomer on the singlet potential energy surface, which corresponds to the species resulting from a hydrogen migration in the P^+-PH_3 complex, lies 127.3 kcal/mol below the reactants level, $P^+(^1D) + PH_3(^1A_1)$. On the triplet surface, on the other hand, the P^+-PH_3 ion−molecule complex is the most stable isomer, 84.4 kcal/mol below $P^+(3P) + PH_3(^1A_1)$. Various reaction paths for both the molecular and atomic hydrogen elimination have been fully characterized. For both spin multiplicities the H_2 abstraction is found to be favored with respect to H abstraction, in full agreement with available experimental data. Finally, we have also discussed the hydrogen and/or charge-transfer reaction between singlet ^1D and triplet ^3P states of P^+ with phosphine.

1. Introduction

Gas-phase ion chemistry is a broad field with many applications and implications in various branches of chemistry.[1] The continuous development of techniques for determining reaction rate coefficients and product distribution is moving forward hand-in-hand with the advancement of accurate computational strategies. And both are stimulated by the growing interest of the species generated and the need of data to substantiate quantitative ion chemical models that describe trends in reactivity, insights into reaction mechanisms, and thermodynamic data such as proton affinities and heats of formation of molecules (including radicals) that are difficult to obtain by others means.[2] One interesting example of this is the study of molecules relevant for the determination of the chemical composition of the interstellar media. Although currently a third of the known astrophysical molecules are uncommon species that would be rather short-lived in the terrestrial enviroment,[3] it is expected that spectroscopic satellites will permit the study of infrared emission and absorption of many other molecules. Nowadays, many potential candidates, including polycyclic aromatic hydrocarbons[4] and molecules containing third-row elements,[5] have been proposed.

Within this context the ion−molecule gas-phase chemistry of the phosphorus cation has been the subject of a considerable amount of research.[6−38] In particular, we have carried out a systematic search of the likely exothermic channels of the reactions of $P^+(^3P)$ with several hydrides[25−28,33−35] (CH_4, NH_3, OH_2, FH, SiH_4, SH_2, and ClH) and other neutral species such as C_2, acetylene, and methanol.[30−32] It is hoped that this series of papers will contribute not only to the understanding of the interstellar production of phosphorus compounds but also to the insight into the general trends of the gas-phase ion chemistry of phosphorus.

In the present paper a theoretical study of the reaction of both $P^+(^1D)$ and $P^+(^3P)$ with PH_3 is carried out. The structure and stabilities of the stable structures on both singlet and triplet potential energy surfaces are characterized. We employed the highly accurate G2 methodology[39−41] to determine the energetics of the stationary points encountered on both PESs. The proton affinities of the singlet and triplet H_2PP and HPPH species are also discussed.

TABLE 1: G2 Total Energies (in hartrees) and G2 Relative Energies (ΔE_{G2} in kcal/mol), with Respect to $P^+(^3P) + PH_3(^1A_1)$, for the Intermediates and Transition States of the Singlet and Triplet $[H_3, P_2]^+$ PESs[a]

species	E_{G2}	ΔE_{G2}	$\langle S^2 \rangle$
$P^+(^3P) + PH_3$	−683.113 32	0.0	2.000
1 (triplet)	−683.247 81	−84.4	2.021
2-anti (triplet)	−683.224 07	−69.5	2.029
2-gauche (triplet)	−683.216 82	−64.9	2.023
3 (triplet)	−683.163 39	−31.4	2.021
TS **1**/**2** (triplet)	−683.190 08	−48.2	2.070
TS **1**/IM (triplet)	−683.163 85	−31.7	2.023
TS **2**/**3** (triplet)	−683.158 92	−28.6	2.035
1 (singlet)	−683.211 47	−61.6	
2 (singlet)	−683.276 44	−102.3	
TS **1**/**2** (singlet)	−683.205 05	−57.6	
TS **2**/H_2 (singlet)	−683.212 65	−62.3	

[a] For the triplets the expectation value of S^2 is also given.

2. Methods

As noted above, we used the G2 methodology, with two slight modifications. Structures were optimized at the MP2/6-311G(d,p), instead of at the MP2/6-31G(d) level of theory. Since we deal with transition states involving H atoms, polarization functions for hydrogen, and not only for heavy atoms, should be included. Also, frequencies were calculated at the MP2/6-311G(d,p) level instead of at the proposed HF/6-31G(d) level of theory. Hence, the zero-point vibrational energy (ZPVE) was obtained at the MP2/6-311G(d,p) level after scaling by 0.94 as recommended.[42] Apart from these two modifications, we have followed the G2 methodology closely.

All calculations have been performed using the GAUSSIAN 92 and GAUSSIAN 94 suite of programs.[43,44] The optimized Cartesian coordinates of all the stationary points discussed in this paper can be found in Tables 1 and 2 of the Supporting Information.

G2 energies can be found in Table 1. The relative stability of each minimum was calculated with respect to the reactants.

† On leave from Dpto de Química, Fac. de Ciencias Nat. y Mat., Universidad de Oriente, Avda. Patricio Lumumba s/n, 90500 Santiago de Cuba, Cuba.

⊗ Abstract published in *Advance ACS Abstracts,* February 1, 1997.

S1089-5639(96)02357-2 CCC: $14.00

TABLE 2: Bonding Properties (in au) at the Bond Critical Point for the Local Minima of the Singlet and Triplet $[H_3, P_2]^+$ PESs[b]

	P−P			P(1)−H			P(2)−H		
species	$\rho(r_c)$	$\nabla^2\rho(r_c)$	$H(r_c)$	$\rho(r_c)$	$\nabla^2\rho(r_c)$	$H(r_c)$	$\rho(r_c)$	$\nabla^2\rho(r_c)$	$H(r_c)$
1 (singlet)	0.1222	−0.1790	−0.0780				0.1731	0.0003	−0.1739
							0.1783	−0.0119	−0.1820
							0.1783	−0.0119	−0.1820
2 (singlet)	0.1447	−0.1105	−0.1385	0.1688	−0.0010	−0.1694	0.1788	−0.0243	−0.1827
							0.1774	−0.0356	−0.1807
1 (triplet)	0.1102	−0.1365	−0.0627				0.1775	0.0007	−0.1801
2-anti (triplet)	0.1170	−0.1563	−0.0673	0.1711	−0.0183	−0.1726	0.1760	−0.0220	−0.1790
							0.1760	−0.0220	−0.1790
2-gauche (triplet)	0.1116	−0.1476	−0.0682	0.1672	−0.0091	−0.1710	0.1767	−0.0217	−0.1798
							0.1767	−0.0217	−0.1798
3 (triplet)[a]	0.1345	−0.2050	−0.0834	0.1708	−0.0185	−0.1727	0.0105	0.0326	0.0013
							0.0105	0.0326	0.0013

[a] For the H−H bond, $\rho(r_c) = 0.2604$, $\nabla^2\rho(r_c) = -1.0575$ and $H(r_c) = -0.2703$. [b] Calculated at the MP2/6-311G(d,p) // MP2/6-311G(d,p) level of theory.

Their salient geometrical parameters can be found in Figure 1. The reaction energy of the exothermic channels has also been evaluated at the G2 level of theory and can be found in Table 3, and their corresponding reactions pathways have been outlined in Figure 2.

We have explored the bonding characteristics of these complexes by means of Bader's topological analysis[45] of the charge density, $\rho(\mathbf{r})$, and its Laplacian, $-\nabla^2\rho(\mathbf{r})$, of the MP2/6-311G(d,p) electron densities using the AIMPAC series of programs.[46] Plots of $-\nabla^2\rho(\mathbf{r})$ for all the minima are depicted in Figure 1 of the Supporting Information. Properties[45−48] of the bond critical point (r_c), such as $\rho(r_c)$, $-\nabla^2\rho(r_c)$, and the value of the energy density $H(r_c)$ for the P−P and P−H bonds of all the minima are found in Table 2. A bond critical point with a positive value of $-\nabla^2\rho(r_c)$ can be interpreted as a point for which the electron charge is locally depleted, whereas a negative value implies that the electronic charge is locally concentrated around such point. Hence, the shape of the Laplacian can be used to characterize the nature of a bond. In this sense, if zones with negative Laplacian are linking two nuclei, we speak about shared interactions between them, since it is common to covalent bonds. However, zones with electronic charge depletion linking the nuclei are typical of ionic or van der Waals molecules and are referred to as closed shell interactions.[45] The value of $\rho(r_c)$ can give an idea of the strength of a bond and for a given pair of atom can also be used as an indicator of their bond order,[47] and the value of the energy density at the bond critical point can also serve to detect covalency in a bond[48] (covalent if $H(r_c) < 0$, and ionic if $H(r_c) > 0$).

Atomic charges have been evaluated with the MP2/6-311G(d,p) wave function by means of two methods: Mulliken and natural bond orbital.[49] Second-order interaction energies between donor ϕ_i and acceptor ϕ_j natural bond orbitals have been calculated as

$$\phi_i \rightarrow \phi_j = \frac{2F_{ij}^{\ 2}}{E_i - E_j}$$

with $F_{ij} = \langle\phi_i|\hat{F}|\phi_j\rangle$, where $\hat{F}$ is the Fock operator and E_i and E_j are the orbital energies of the donor and the acceptor, respectively. We have used the GAUSSIAN 92,[43] GAUSSIAN 94,[44] and NBO[50] programs to carry out these calculations. A complete list of calculated atomic charges is found in Table 3 of the Supporting Information.

3. Structures, Bonding, and Stabilities

Figure 1 depicts the salient geometrical features of the various stable structures found on both the singlet (upper half of Figure 1) and the triplet (lower half of Figure 1) potential energy surfaces of the $[H_3, P_2]^+$ system. Their Cartesian coordinates can be found in Tables 1 and 2 of the Supporting Information. All the structures outlined in Figure 1 lie energetically below their corresponding reactants energy level, namely, $P^+(^1D) + PH_3(^1A_1)$ for the singlets and $P^+(^3P) + PH_3(^1A_1)$ for the triplets. We will now highlight some of their bonding and stability features according to the following order: first, isomers **1** (triplet) and **1** (singlet), which are the ion−molecule complexes formed along the entrance channels of the $P^+(^3P)$ and $P^+(^1D) + PH_3(^1A_1)$ reactions, respectively, then isomers **2**-anti (triplet), **2**-gauche (triplet), and **2** (singlet), which correspond to species formed through a hydrogen shift, and finally we shall discuss isomer **3** (triplet), which can be best viewed as a complex between $HPP^+(^3A')$ and a hydrogen molecule.

The ion−molecule complexes **1** (triplet) and **1** (singlet) have been discussed in detail in an earlier publication.[51] Nevertheless, it is worth noting further that the NBO analysis of the singlet ion−molecule complex reveals a noticeable charge-transfer interaction between the doubly occupied 3p orbital of the terminal P atom with the σ^*_{P-H} with an NBO interaction energy[49] of 14.3 kcal/mol, while for the triplet ion−molecule complex, this interaction energy is only 5.0 kcal/mol. This is consistent with both the shorter P−P bond length and the smaller PPH bond angle of the singlet structure **1** with respect to the triplet structure **1**. Recall that this sort of interaction has been recognized to be crucial for rationalizing the geometrical distortions of metal carbene complexes[52] and for explaining the hyperconjugative stabilization of silylium cations.[53]

The migration of a hydrogen over the terminal P atom (P(2), P(1) H shift) in isomer **1** (singlet) leads to the planar structure **2** (singlet). This turns out to be the absolute energy minimum of both PESs. It also bears the shortest P−P bond length of all the isomers studied, 2.005 Å, suggestive of a double P−P bond. Indeed, our predicted P−P bond length for isomer **2** (singlet) compares well with the P−P bond lengths determined by X-ray diffraction for substituted *trans*-diphosphenes,[54−56] which are found to lie within the 2.00−2.03 Å range. Also, earlier theoretical calculations on *trans*-diphosphene have led to P−P double bond lengths of 2.068 Å at the MCSCF/3-21G(d) level of theory[57] and 2.004 Å at the HF/6-31G(d,p) level of theory,[58] which bracket narrowly our value of 2.005 Å. The double bond nature of the P−P bond in isomer **2** (singlet) is confirmed further by inspection of the topological properties of the bond critical point (r_c) shown in Table 2. Thus, the electronic charge density at the bond critical point, $\rho(r_c)$ of the P−P bond is substantially larger for **2** (singlet) than for **1** (singlet). Accordingly, the energy density at the bond critical point, $H(r_c)$, is also more

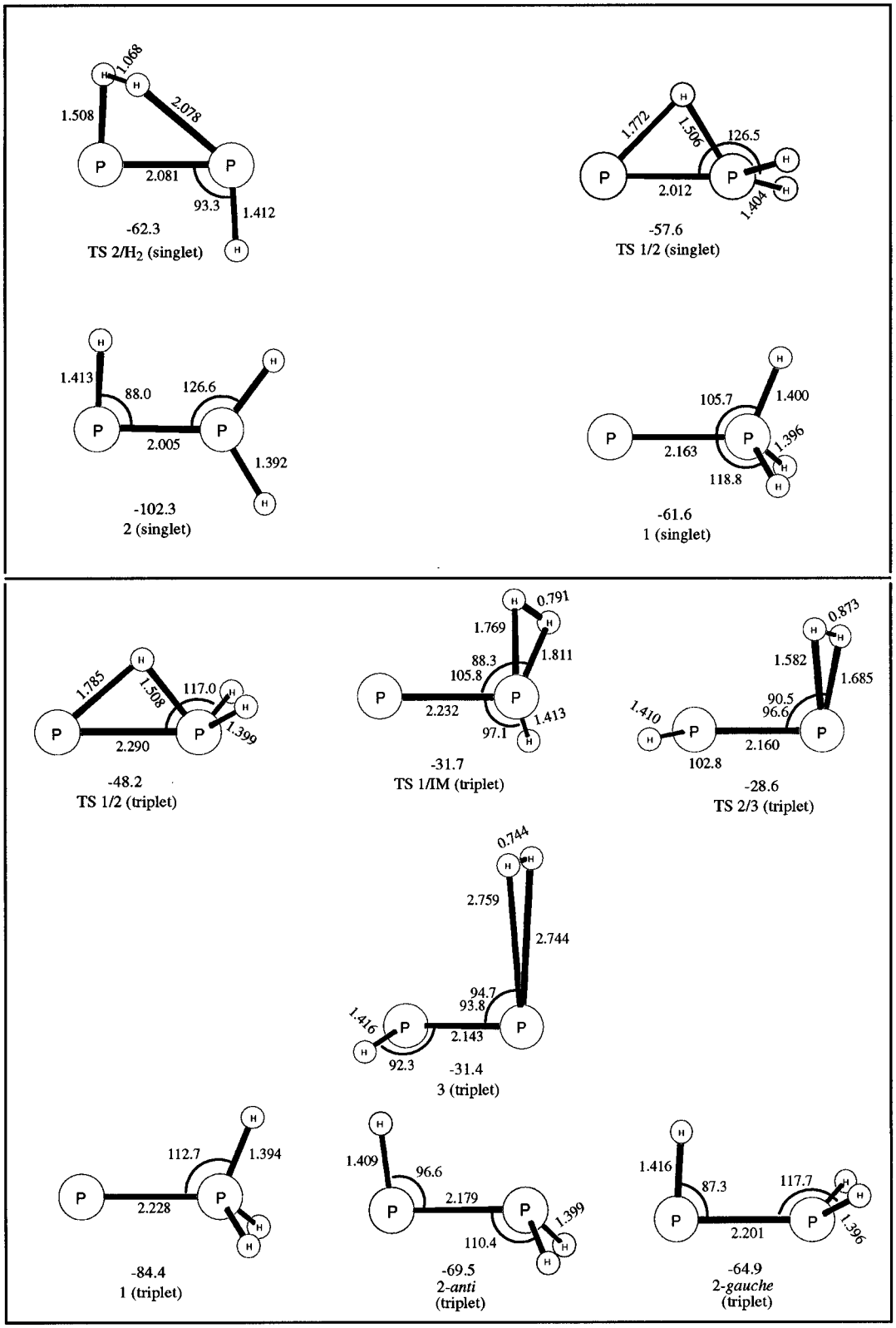

Figure 1. MP2/6-311G(d,p) selected geometries data and relative stabilities (G2 level, kcal/mol), with respect to $P^+(^3P) + PH_3(^1A_1)$, of the intermediates and transition states of the singlet and triplet $[H_3, P_2]^+$ PESs. Bond lengths are in angstroms and bond angles in degrees.

negative for **2** (singlet) than for **1** (singlet), indicating the P−P is more covalent[51] for **1** (singlet) than for **2** (singlet). Notice that $H(r_c)$ for P−P of **2** (singlet) is near twice that of **1** (singlet). In addition, the NBO analysis assigns a double P−P bond to isomer **2** (singlet) and shows that the P(1)−H bond is mainly made of the in-plane 3p orbital of the P(1) atom with the 1s of the hydrogen, which is consistent with the HP(1)P(2) bond angle being close to 90°.

On the triplet potential energy surface, the hydrogen shift from P(2) to P(1) in the ion−molecule complex **1** (triplet) leads to the nonplanar isomers **2**-anti (triplet) and **2**-gauche (triplet) depicted in Figure 1. Indeed, contrary to the singlet surface, the hydrogen shift destabilizes the system. Thus, **2**-anti (triplet) and **2**-gauche (triplet) are, respectively, 14.9 and 19.5 kcal/mol more unstable than **1** (triplet) while on the singlet surface **2** (singlet) is found to be 40.7 kcal/mol more stable than **1** (singlet)

TABLE 3: G2 Total Energies (in hartrees) and G2 Relative Energies (ΔE_{G2} in kcal/mol) for the Reactants and Products of $P^+ + PH_3$ Reactions (Singlet and Triplet States for P^+)

species	E_{G2}	ΔE_{G2}
$P^+(^1D) + PH_3(^1A_1)$		
$P^+(^1D) + PH_3(^1A_1)$	−683.073 48	0.0
$PPH^+(^1A') + H_2(^1\Sigma_g^+)$	−683.219 93	−91.9
$PPH_2^+(^2A') + H(^2S)$	−683.148 99	−47.4
$HPPH^+(^2A') + H(^2S)$	−683.132 85	−37.2
$PH_2^+(^1A_1) + PH(^1\Sigma^+)$	−683.081 19	−4.8
$PH_3^+(^2A_1)^a + P(^2P)$	−683.076 67	−2.0
$P^+(^3P) + PH_3(^1A_1)$		
$P^+(^3P) + PH_3(^1A_1)$	−683.113 32	0.0
$PPH^+(^3A') + H_2(^1\Sigma_g^+)$	−683.158 91	−28.6
$PPH_2^+(^2A') + H(^2S)$	−683.148 99	−22.4
$HPPH^+(^2A') + H(^2S)$	−683.132 85	−12.2
$PH_2^+(^1A_1) + PH(^3\Sigma^-)^a$	−683.120 27	−4.4
$PH_3^+(^2A_1)^a + P(^2P)$	−683.076 67	+23.1

[a] Taken from ref 41.

at the G2 level of theory. From the structural point of view, both **2**-anti (triplet) and **2**-gauche (triplet) are rationalized simply by invoking an sp^3 hybridization of P(2) and an equal sharing of the spin density between the two P atoms. This can be seen by inspection of the topological analysis data of the electron density, collected in Table 2, which are indicative of a singly bound P−P backbone with three almost alike P−H bonds arranged as either anti or gauche configurations. Notice that our MP2/6-311G(d,p) optimum P−P bond length of 2.201 Å in the **2**-gauche (triplet) structure is very close to the HF/6-31G(d,p) optimum bond length of the ^3B state of the *trans*-diphosphene,[58] which has a P−P single bond.

Isomer **3** (triplet) is best viewed as a complex between the $HPP^+(^3A')$ and the hydrogen molecule. Both Mulliken and natural bonding populations analyses predict that the positive charge is borne by the HPP^+ moiety and that the H_2 moiety remains neutral. On the other hand, the large intermoiety distance and the positive value of $H(r_c)$ (0.0013) at the P(2)−H bond critical point (see Table 2) reveal the largely electrostatic nature of the intermoiety interaction. Finally, it is worth mentioning that the P−P bond length is shorter than those of isomers **2**-anti (triplet) and **2**-gauche (triplet). A trend akin to that found for the adducts of the H_2 with the triplet $[H_2, Si, P]^+$ system[35] should be attributed to the $\sigma_{P1-H} \rightarrow n^*_{3p(P2)}$ interaction, which for the isomer **3** (triplet) amounts to 4.3 kcal/mol. Notice, also, that the ion−molecule complex **3** (triplet) is the least stable structure of both singlet and triplet $[H_3, P_2]^+$ systems, as shown in Table 1.

4. Proton Affinities of H_2PP and HPPH

Proton affinity is an important property in gas-phase chemistry in general, and it is of special interest to elucidate likely interstellar molecules. It should be remembered that proton-exchange reactions play a central role in interstellar chemistry.[59] Proton affinities (PA's) for both singlet and triplet H_2PP and HPPH species are shown in Table 4. The PA's were computed by means of

$$PA(T) = -\Delta E_e - \Delta E_v - \Delta E_r + (5/2)RT$$

where ΔE_e is the electronic energy difference, ΔE_v the vibrational energy difference, and ΔE_r the rotational energy difference between the neutral and protonated species. The values of Table 4 correspond to PA at 298 K. In the H_2PP isomer, protonation can take place either on the terminal phosphorus atom or in the central phosphorus atom. It is worth mentioning that for the singlet state, protonation of H_2PP will take place preferentially on the terminal P atom, since its proton affinity is predicted to be 53.5 kcal/mol larger than that of the central P atom, as shown in Table 4. However, for the triplet surface, it is the central P atom that has a larger PA than the terminal P atom, although the difference is only of 4.5 kcal/mol. On the other hand, for the HPPH isomer the predicted PA's for the singlet and triplet states are rather similar (see Table 4), being only 1.1 kcal/mol larger for the triplet state. Recall that the PA of HPPH (^1A_g) has been calculated earlier[58] at the HF, MP2, and MP3 levels of theory with a basis set of double-ζ quality plus polarization. Their best value is 183.0 kcal/mol, only 2.5 kcal/mol smaller than our G2 estimate of 185.5 kcal/mol (see Table 4). This slight increase of the PA with increasing quality of the level of theory has been found earlier for other noncyclic phosphorus-containing compounds.[28,33] Notice that for cyclic species the opposite trend is found.[60]

5. Reaction Mechanisms

The reaction of P^+ with PH_3 has been studied experimentally by Smith et al.,[61] who used the selected ion flow tube (SIFT) technique. They detected two different channels

$$P^+ + PH_3 \rightarrow (P_2H)^+ + H_2 \quad (1)$$

$$P^+ + PH_3 \rightarrow (P_2H_2)^+ + H \quad (2)$$

with the following product distribution: 0.62 for $(P_2H)^+$, 0.12 for $(P_2H_2)^+$, and 0.26 for the charge-transfer process leading to PH_3^+. The rate coefficient for this reaction is relatively high, 1.2×10^{-9} cm^3 s^{-1}. Earlier, Thorne et al.,[62] using the ion cyclotron resonance (ICR) technique, found the same reaction products but a different distribution, namely, 0.85 for $(P_2H)^+$, 0.09 for $(P_2H_2)^+$, and 0.06 for the charge-transfer channel. These product distribution data clearly indicate that reaction 1 is dominant. Indeed, we have found (see Table 3) that on both the singlet and triplet potential energy surfaces, reactions 1 and 2 are exothermic. However, the charge-transfer process from the ion to the molecule $P^+ + PH_3 \rightarrow P + PH_3^+$ is definitely endothermic on the triplet surface (by 23.1 kcal/mol at the G2 level of theory), while on the singlet the predicted figure, 2.0 kcal/mol exothermic, lies within the errors bars of the procedure used to calculated it.[41] Nevertheless, we have found that the hydrogen transfer reaction

$$P^+ + PH_3 \rightarrow (PH_2)^+ + PH \quad (3)$$

is also slightly exothermic on both, the singlet and triplet, surfaces by 4.8 and 4.4 kcal/mol, respectively, as shown in Table 3. For the sake of completeness we shall consider reaction 3 along with reactions 1 and 2 in our study. Notice that all the mechanisms discussed in this section involve intermediates and transition states all lying below the energy level of the reactants. Henceforth, they will be useful pieces of information for astrochemists, since interstellar chemical processes must have low (or zero) activation energies and must also be exothermic to proceed under the low-density and low-temperature conditions of the interstellar space.[63] Nevertheless, it should be mentioned that nowadays these data are of limited value for astrochemists, for PH_3 has not yet been detected in either the interstellar or circumstellar regions,[64] although it is known to exist in the Jupiter's atmosphere.[65]

5.1. Singlet PES. The formation of the ion−molecule complex **1** (singlet) can be considered as the first step in the $P^+(^1D) + PH_3(^1A_1)$ reaction. It is exothermic by 86.6 kcal/mol and proceeds without a transition state at the G2 level of

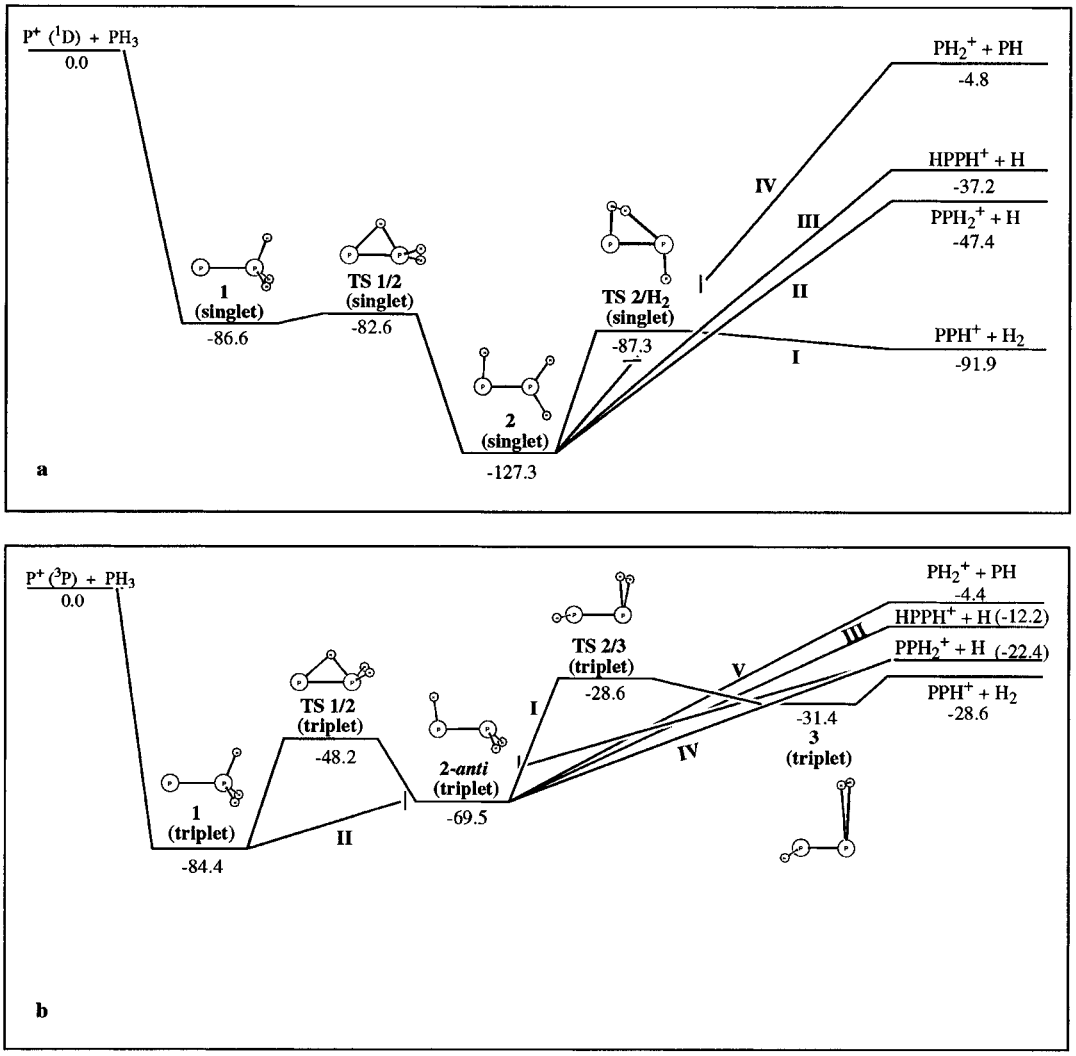

Figure 2. Schematic representation of the different reaction mechanisms calculated at the G2 level of theory (values in kcal/mol): (a) $P^+(^1D) + PH_3(^1A_1)$ reaction; (b) $P^+(^3P) + PH_3(^1A_1)$ reaction.

TABLE 4: Proton Affinities, PA, in kcal/mol, for the Singlet and Triplet (in Parentheses) Spin States of H_2PP and HPPH, and Their Singlet−Triplet Energy Gaps, Δ_{T-S}, in kcal/mol, at the G2 Level of Theory

	H_2PP		
	terminal P	central P	HPPH
PA	233.7	192.1	185.5
	(180.2)	(196.6)	(186.6)
Δ_{T-S}	−18.7		35.4

theory. Furthermore, this ion−molecule complex rearranges to isomer **2** (singlet) by a P(2), P(1) H shift. The latter process goes through transition state TS **1**/**2** (singlet), with a small activation energy, namely, 4.0 kcal/mol, and leads to the most stable isomer of the singlet PES. Notice that the whole process runs well below the reactants energy level. Then isomer **2** (singlet) can break apart, either by releasing molecular hydrogen or atomic hydrogen or by cleavage of the P−P bond. Each of these reaction pathways will be discussed in turn.

Abstraction of H_2. Reaction pathway I of Figure 2a outlines this mechanism. It turns out to be the most exothermic process on the singlet PES, with the products lying 91.9 kcal/mol below the reactants level. This agrees with the experiments[61,62] in the sense that $(P_2H)^+$ is the most abundant product of the $P^+ + PH_3$ reaction. The transition state of this reaction, TS **2**/H_2 (singlet), lies 40 kcal/mol above the isomer **2** (singlet) and has a long length for the H−H forming bond. Hence, it is predicted that the resulting H_2 will be vibrationally excited.[66,67] This transition state corresponds to a 1,2-elimination reaction, and it is structurally similar to the transition state of 1,2-elimination of molecular hydrogen from the singlet P_2H_4 molecule.[57] Also notice that the $PPH^+(^1\Sigma)$ product molecule has a P−P triple bond, as suggested by its short P−P bond length of 1.908 Å and further by the natural bonding analysis. The latter reveals that the central phosphorus (P(2)) atom is sp hybridized and that the terminal phosphorus (P(1)) atoms bears a lone pair, which correspond to its 3s atomic orbital. This molecule has a rather large dipole moment, namely, 6.73 D at the MP2/6-311G-(d,p) level of theory, which might facilitate its detection.

Abstraction of H. Indeed, two species can be formed starting from isomer **2** (singlet) by abstraction of atomic hydrogen, namely, $PPH_2^+(^2A')$ and $HPPH^+(^2A')$, the former being 10.2 kcal/mol more stable than the latter. We were unable to find any transition state for these reactions, which led us to think that they may proceed without an activation barrier. To assess this hypothesis, we carried out geometry optimizations for $HPPH_2^+$ at various fixed P−H distances at the MP2/6-311G-(d,p) level of theory. The results show a monotonic increase of the energy until either $PPH_2^+(^2A')$ or $HPPH^+(^2A')$ is reached. The whole mechanisms for both reactions are depicted as pathways II and III in Figure 2a. Notice that both pathways lie below the reactants energy level, and correspond to exothermic reactions, by 47.4 and 37.2 kcal/mol, respectively, with respect to the reactants, but they are, respectively, 44.9 and 54.7 kcal/

mol above the most exothermic products (see Table 3). This also agrees with the experimental fact of $(P_2H_2)^+$ being the second most abundant product of the $P^+ + PH_3$ reaction.[61,62]

P−P Bond Cleavage. As outlined by pathway IV of Figure 2a, breaking the P−P bond of isomer **2** (singlet) leads to the least stable fragmentation products, $PH_2^+(^1A_1) + PH(^1\Sigma)$, on the singlet potential energy without an activation barrier. However, it is worth noting that the products lie only 4.8 kcal/mol below the reactants level but 32.4 kcal/mol above the next less stable fragmentation products, namely, $HPPH^+(^2A')$ + $H(^2S)$. Recall that the whole process involves not only a hydrogen transfer from PH_3 to P^+ but also the transfer of charge in the opposite direction. This latter process has already begun at isomer **1** (singlet), as indicated by its natural atomic charges (see Table 3 of the Supporting Information), which assigns a 0.59*e* to the PH_3 moiety in isomer **1** (singlet).

5.2. Triplet PES. For the singlet PES, on the triplet PES, formation of an ion−molecule complex, **1** (triplet) in this case, is also the first step in the reaction of the phosphorus cation with $PH_3(^1A_1)$. The energies of the various products studied, with respect to the reactants level, are shown in Table 3 and their reactions pathways outlined in Figure 2b. Notice that, unlike the singlet PES, we have now considered the fragmentation of both the P^+-PH_3 ion−molecule complex **1** (triplet) and the **2**-anti (triplet) isomer, since the energy barrier connecting the two structures is now 36.2 kcal/mol, which is to be compared with 4.0 kcal/mol for the analogous singlet case. Therefore, it seems likely that the ion−molecule **1** (triplet) will have a considerably longer lifetime than **1** (singlet). However, we have been able to characterized only the hydrogen atom abstraction reaction from **1** (triplet), as shown in Figure 2b, the rest of the fragmentation reactions occurring from isomer **2** (triplet). However, it is worth noting that a transition state TS **1**/IM (triplet) (see Figure 1), corresponding to the 1,1-elimination of H_2 from the ion−molecule complex **1** (triplet), has been characterized, but it has been found to lie below the energy level of the products. Therefore, it is expected that an ion−molecule (IM) complex exists, with H_2 on top of the central phosphorus atom, from which the abstraction of H_2 will likely take place without an activation barrier. Extensive searching of the PES at the MP2/6-311G(d,p) level of theory failed to locate such an adduct. Nevertheless, it should not be ruled out that higher levels of theory will succeed in finding it.

Abstraction of H_2. It is the most exothermic reaction. Inspection of pathway I of Figure 2b reveals that it takes place in two steps from isomer **2** (triplet) and that this process is the least favored kinetically. The first step consists of the formation of the HPP^+-H_2 ion−molecule complex **3** (triplet) through the transition state TS **2**/**3** (triplet). This step requires an activation energy of 40.9 kcal/mol from **2** (triplet) and leads to the weakly bound ion−molecule complex **3** (triplet), only 2.8 kcal/mol below the energy of the fragmentation final products, HPP^+ and H_2. The latter step proceeds without an activation barrier. Notice that, contrary to the singlet PES, the H_2 molecule will now be released in its vibrational ground state, since the H−H distance is close to the H_2 equilibrium bond length. The resultant $HPP^+(^3A')$ species is also worth a short discussion. It has a bent geometry, with a bond angle of 113.8° and a P−P bond length of 2.043 Å, suggestive of a double bond. Indeed, this point is confirmed further by inspection of the NBO data, which also reveal an sp^2 hybridized central phosphorus atom. The spin density is equally shared by both of the phosphorus atoms, the singly occupied molecular orbitals (SOMO) corresponding to the out-of-plane 3p orbital of the terminal P and one of the sp^2 hybrid orbitals of the central P. The former has an interaction energy of 8.77 kcal/mol with the antibonding σ_{P-H} orbital. This is reflected in the longer P−H bond length of this electronic state, 1.412 Å, with respect to the singlet state, 1.405 Å.

Abstraction of H. As outlined in reaction pathways II−IV of Figure 2b, the reaction products $PPH_2^+(^2A') + H(^2S)$ can also be reached in the triplet PES. However, it is worth mentioning that they are less exothermic than for the singlet PES, namely, 22.4 and 12.2 kcal/mol, respectively, as shown in Table 3. This simply reflects the energy gap of 25.0 kcal/mol between the triplet and singlet phosphorus ions[51] at this level of theory, which should be compared with the experimental value[68] of 24.92 kcal/mol.

P−P Bond Cleavage. On the triplet PES the cleavage of the P−P bond of isomer **2** (triplet) yields $PH_2^+(^1A_1) + PH(^3\Sigma^-)$, a reaction that proceeds without an activation barrier and that is only 4.4 kcal/mol exothermic. The charge-transfer process involved in this reaction is developed at the **2** (triplet) intermediate further than on the singlet PES, since the calculated natural charges on its PH and PH_2 moieties, shown in Table 3 of the Supporting Information, are 0.37*e* and 0.63*e*, respectively, which are to be compared with their corresponding values of 0.48*e* and 0.52*e* for the singlet species **2** (singlet). Notice also that this reaction yields both PH_2^+ and PH in their ground states, contrary to its analogue of the singlet PES, which yields PH in its first excited state ($^1\Sigma^+$).

6. Concluding Remarks

The singlet and the triplet potential energy surfaces of the $[H_3, P_2]^+$ system have been studied thoroughly. Various stables structures with energies lower than $P^+(^1D) + PH_3(^1A_1)$ and $P^+(^3P) + PH_3(^1A_1)$ have been characterized on the singlet and triplet surfaces, respectively. These structures have been confirmed to be accessible under interstellar medium conditions, since the transition states of their corresponding reaction mechanisms lie energetically below the reactants level. In particular, it is pointed out that the formation of the ion−complex P^+-PH_3 provides a significant amount of energy to overcome additional energy barriers, since under the low-density conditions of the interstellar medium the energy cannot dissipate. Notice, however, that we have not considered the effect of the crossing between the singlet and triplet potential energy surfaces. Although this is expected to represent a minor channel for the reaction of P^+ with PH_3, it might modify slightly the relative yield of the products. The global minimum found on the singlet $[H_3, P_2]^+$ PES is **2** (singlet), a species resulting from transferring one of the hydrogens of the PH_3 to the phosphorus cation. This **2** (singlet) isomer has a P−P bond length that compares well with the experimental P−P double bond lengths of a number of diphosphenes. Notice that **2** (singlet) is 40.7 kcal/mol more stable than the ion−molecule complex **1** (singlet). However, on the triplet surface, the hydrogen shift from P(2) to P(1) in the ion−molecule complex destabilizes the system by 14.9 kcal/mol, yielding the **2**-anti (triplet) isomer, which has a single P−P bond. Rotation around this bond leads to **2**-gauche (triplet), which is only 4.6 kcal/mol more unstable than **2**-anti (triplet).

We have also found a stable adduct between H_2 and the HPP^+ on the triplet PES with its intramolecular interaction largely dominated by electrostatics and that is 31.4 kcal/mol more stable than $P^+(^3P) + PH_3(^1A_1)$.

The most exothermic channel found in this work corresponds to the abstraction of molecular hydrogen, either through a 1,2-elimination from the singlet **2** (singlet) structure or through a 1,1-elimination from the **2**-anti (triplet) structure. The latter, in fact, leads first to the ion−molecule **3** (triplet), and then H_2

elimination proceeds without an activation barrier. Atomic hydrogen elimination is predicted to proceed without an activation barrier on both studied potential energy surfaces. However, the hydrogen shift from P(2) to P(1) takes places with a considerable activation of 36.2 kcal/mol on the triplet PES, while it requires only 4.0 kcal/mol activation energy on the singlet PES. Finally, it should be mentioned that our calculations agree with the experimentally known product distribution for the $P^+ + PH_3$ reaction.

Acknowledgment. This research has been supported by the University of the Basque Country (Euskal Herriko Unibertsitatea) and the Basque government (Eusko Jaurlaritza) Grant No. GV 203.215-0049/94, and the Basque Provintial Government of Guipuzkoa (Gipuzkoako Foru Aldundia). X.L. thanks the Basque government for a grant, and E.M.C. thanks the Spanish A.E.C.I. for financial aid and support.

Supporting Information Available: Tables I−IV listing Cartesian coordinates, atomic charges, imaginary frequencies, and normal mode coordinates of $[H_3, P_2]^+$ and Figure 1 showing contour maps for $[H_3, P_2]^+$ intermediates (5 pages). Ordering information is given on any current masthead page.

References and Notes

(1) Adams, N. G., Babcock L. M., Eds. *Advances in Gas Phase Ion Chemistry*, Jai Press: Greenwich, CT, 1992.
(2) Williams, I. H. *Annu. Rep. Prog. Chem*. **1988**, *27*, 85.
(3) Smith, D. *Chem. Rev*. **1992**, *92*, 1473.
(4) Cook, D. J.; Schlemmer, S.; Balucami, N.; Wagner, D. R.; Steiner, B.; Saykally, R. J. *Nature* **1996**, *380*, 227.
(5) Turner, B. E. *Space Sci. Rev*. **1989**, *51*, 235.
(6) Holtz, D.; Beauchamp, J. L.; Eyler, J. R. *J. Am. Chem. Soc*. **1970**, *92*, 7045.
(7) Trinquier, G. *J. Am. Chem. Soc.* **1982**, *104*, 6969.
(8) Ha, T. K.; Nguyen, M. Y.; Ruelle, P. *Chem. Phys*. **1984**, *87*, 23.
(9) Nguyen, M. Y.; McGinn, M. A.; Hegarty, A. F. *J. Am. Chem. Soc*. **1985**, *107*, 8029.
(10) Nguyen, M. Y. *Chem. Phys*. **1987**, *117*, 91.
(11) Nguyen, M. Y.; Ha, T. K. *Chem. Phys*. **1989**, *131*, 245.
(12) Allen, T. L.; Scheiner, A. C.; Yamaguchi, Y.; Schaefer, H. F., III *Chem. Phys. Lett*. **1985**, *121*, 154.
(13) Berkowitz, J.; Curtiss, L. A.; Gibson, S. T.; Greene, J. P.; Hillhouse, G. J.; Pople, J. A. *J. Chem. Phys*. **1986**, *84*, 375.
(14) Bachrach, S. M. *J. Comput. Chem*. **1989**, *10*, 392.
(15) Maclagan, R. G. A. R. *Chem. Phys. Lett*. **1989**, *163*, 349.
(16) Maclagan, R. G. A. R. *J. Phys. Chem.* **1990**, *94*, 3373.
(17) Glaser, R.; Horan, C. J.; Choy, G. S. C.; Harris, B. L. *J. Phys. Chem.* **1992**, *96*, 3689.
(18) Glaser, R.; Horan, C. J.; Haney, P. E. *J. Phys. Chem.* **1993**, *97*, 6607.
(19) Karna, S. P.; Bruna, P. J.; Grein, F. *Chem. Phys*. **1988**, *123*, 85.
(20) Essefar, M.; Luna, A.; Mo, O.; Yáñez, M. *Chem. Phys. Lett*. **1993**, *209*, 557.
(21) Luna, A.; Yáñez, M. *J. Phys. Chem.* **1993**, *97*, 10659.
(22) Essefar, M.; Luna, A.; Mo, O.; Yáñez, M. *J. Phys. Chem.* **1993**, *97*, 6607.
(23) Essefar, M.; Luna, A.; Mo, O.; Yáñez, M. *J. Phys. Chem.* **1994**, *98*, 8679.
(24) Essefar, M.; Luna, A.; Mo, O.; Yáñez, M. *Chem. Phys. Lett*. **1994**, *223*, 240.
(25) Largo, A.; Flores, J. R.; Barrientos, C.; Ugalde, J. M. *J. Phys. Chem.* **1991**, *95*, 170.
(26) Largo, A.; Redondo, P.; Barrientos, C.; Ugalde, J. M. *J. Phys. Chem.* **1991**, *95*, 5443.
(27) Largo, A.; Flores, J. R.; Barrientos, C.; Ugalde, J. M. *J. Phys. Chem.* **1991**, *95*, 6553.
(28) Redondo, P.; Largo, A.; Barrientos, C. and Ugalde, J. M. *J. Phys. Chem.* **1991**, *95*, 4318.
(29) Largo, A.; Barrientos, C. *J. Phys. Chem.* **1991**, *95*, 9864.
(30) Largo, A.; Barrientos, C.; Lopez, X.; Ugalde, J. M. *J. Phys. Chem.* **1994**, *98*, 3985.
(31) Largo, A.; Barrientos, C.; Lopez, X.; Cossío, F. P.; Ugalde, J. M. *J. Phys. Chem.* **1995**, *99*, 6432.
(32) Cruz, E. M.; Lopez, X.; Ugalde, J. M.; Cossío, F. P. *J. Phys. Chem.* **1995**, *99*, 12170.
(33) Lopez, X.; Ugalde, J. M.; Barrientos, C.; Largo, A.; Redondo, P. *J. Phys. Chem.* **1993**, *97*, 1521.
(34) Lopez, X.; Ayerbe, M.; Ugalde, J. M.; Cossío, F. P. *J. Phys. Chem.* **1995**, *99*, 6812.
(35) Cruz, E. M.; Lopez, X.; Sarobe, M.; Cossío, F. P.; Ugalde, J. M. *J. Comput. Chem*. **1997**, *18*, 9.
(36) Adams, N. G.; McIntosh, B. J.; Smith, D. *Astron. Astrophys*. **1990**, *232*, 443.
(37) Zimmerman, J. A.; Bach, S. B. H.; Watson, C. H.; Eyler, J. R. *J. Phys. Chem.* **1991**, *95*, 98.
(38) Muedas, C. A.; Schröder, D.; Sülzle, D.; Schwarz, H. *J. Am. Chem. Soc.* **1992**, *114*, 7582.
(39) Pople, J. A.; Head-Gordon, M.; Fox, D. J.; Raghavachari, K.; Curtiss, L. A. *J. Chem. Phys*. **1989**, *90*, 5622.
(40) Curtiss, L. A.; Jones, C.; Trucks, G. W.; Raghavachari, K.; Pople, J. A. *J. Chem. Phys*. **1990**, *93*, 2537.
(41) Curtiss, L. A.; Raghavachari, K.; Trucks, G. W.; Pople, J. A. *J. Chem. Phys*. **1991**, *94*, 7221.
(42) Defrees, D. J.; McLean, A. D. *J. Chem. Phys.* **1985**, *82*, 333.
(43) Frisch, M. J.; Trucks, G. W.; Head-Gordon, M.; Gill, P. M. W.; Wong, M. W.; Foresman, J. B.; Johnson, B. G.; Schlegel, H. B.; Robb, M. A.; Replogle, E. S.; Gomperts, R.; Andres, J. L.; Raghavachari, K.; Binkley, J. S.; Gonzalez, C.; Martin, R. L.; Fox, D. J.; Baker, J.; Stewart, J. J. P.; Pople, J. A. *Gaussian 92*, Revision C; Gaussian, Inc.: Pittsburgh, PA, 1992.
(44) Frisch, M. J.; Trucks, G. W.; Schlegel, H. B.; Gill, P. M. W.; Johnson, B. G.; Robb, M. A.; Cheeseman, J. R.; Keith, T. A.; Petersson, G. A.; Montgomery, J. A.; Raghavachari, K.; Al-Laham, M. A.; Zakrzewski, V. G.; Ortiz, J. V.; Foresman, J. B.; Cioslowski, J.; Stefanov, B; Nanayakkara, A.; Challacombe, M.; Peng, C. Y.; Ayala, P. Y.; Chen, W.; Wong, M. W.; Andres, J. L.; Replogle, E. S.; Gomperts, R.; Martin, R. L.; Fox, D. J.; Binkley, J. S.; Defrees, D. J.; Baker, J.; Stewart, J. P.; Head-Gordon, M.; Gonzalez, C.; Pople, J. A. *Gaussian 94*, Revision B.1; Gaussian, Inc.: Pittsburgh, PA, 1995.
(45) Bader, R. F. W. *Atoms in Molecules. A Quantum Theory*; Clarendon Press: Oxford, 1990.
(46) Biegler-König, F. W.; Bader, R. F. W.; Tang, T. *J. Comput. Chem*. **1982**, *3*, 317.
(47) Bader, R. F. W.; Tang, T.; Tal, Y.; Biegler-Köning, F. W. *J. Am. Chem. Soc.* **1982**, *104*, 946. For a review, see the following. Boyd, R. J.; Ugalde, J. M. *Computational Chemistry, Part A*; Fraga, S., Ed.; Elsevier: Amsterdam, 1992.
(48) Biegler-König, F. W.; Bader, R. F. W.; Tang, T. *J. Comput. Chem*. **1980**, *27*, 1924.
(49) (a) Reed, A. E.; Weinstock, R. B.; Weinhold, F. *J. Chem. Phys*. **1985**, *83*, 735. (b) Reed, A. E.; Curtiss, L. A.; Weinhold, F. *Chem. Rev*. **1988**, *88*, 899. (c) Reed, A. E.; Schleyer, P. v. R. *J. Am. Chem. Soc.* **1990**, *112*, 1434.
(50) Glendening, E. D.; Reed, A. E.; Carpenter, J. E.; Weinhold, F. *NBO*, Version 3.1.
(51) Lopez, X.; Irigoras, A.; Ugalde, J. M.; Cossío, F. P. *J. Am. Chem. Soc*. **1994**, *116*, 10670.
(52) France, M. M.; Pietro, W. J.; Hout, R. F., Jr.; Hehre, W. J. *Organometallics* **1983**, *2*, 281.
(53) Xie, Z.; Ban, R.; Benesi, A.; Reed, C. A. *Organometallics* **1995**, *14*, 3933.
(54) Yoshifugi, M.; Shima, I.; Inamoto, W.; Hirotsu, K.; Higuchi, T. *J. Am. Chem. Soc*. **1981**, *103*, 4587.
(55) Cowley, A. H. *Acc. Chem. Res* **1984**, *17*, 386.
(56) Jaud, J; Couret, C.; Escudie, J. *J. Organomet. Chem*. **1983**, *249*, C25.
(57) Schmidt, M. W.; Gordon, M. S. *Inorg. Chem*. **1986**, *25*, 248.
(58) Ito, K.; Nagase, S. *Chem. Phys. Lett*. **1986**, *126*, 531.
(59) Millar, T. J. In *Molecular Astrophysics*; Hartquist, T. W., Ed.; Cambridge University Press: Cambridge, 1990.
(60) Irigoras, A; Cossío, F. P.; Sarasola, C.; Ugalde, J. M. *J. Phys. Chem.* **1996**, *100*, 8758.
(61) Smith, D.; McIntosh, B. J.; Adams, N. G. *J. Chem. Phys*. **1989**, *90*, 6213.
(62) Thorne, L. R.; Anicich, V. G.; Huntress, W. T. *Chem. Phys. Lett*. **1983**, *98*, 162.
(63) Adams, N. G.; Smith, D. In *Astrochemistry*; Vardya, M. S., Tarafdar, S. P., Eds.; D. Reidel Publishing Co.: Dordrecht, Holland, 1987.
(64) Hartquist, T. W.; Williams, D. A. *The Chemically Controlled Cosmos*; Cambridge University Press: Cambridge, U.K., 1995.
(65) Ridgeway, S. T.; Wallace, L.; Smith, G. R. *Astrophys. J*. **1976**, *207*, 1002.
(66) Jensen, J. H.; Morokuma, K.; Gordon, M. S. *J. Chem. Phys*. **1994**, *100*, 1981.
(67) Beijersbergen, J. H. M.; van der Zande, W. J.; Kistemaker, P. G.; Los, J. *J. Phys. Chem.* **1993**, *97*, 11180.
(68) See http://aeldata.phy.nist.gov/nist_atomic_spectra.html.